



The Society shall not be responsible for statements or opinions advanced in papers or discussion at meetings of the Society or of its Divisions or Sections, or printed in its publications. Discussion is printed only if the paper is published in an ASME Journal. Authorization to photocopy for internal or personal use is granted to libraries and other users registered with the Copyright Clearance Center (CCC) provided \$3/article or \$4/page is paid to CCC, 222 Rosewood Dr., Danvers, MA 01923. Requests for special permission or bulk reproduction should be addressed to the ASME Technical Publishing Department.

Copyright © 1998 by ASME

All Rights Reserved

Printed in U.S.A.

## THE INFLUENCE OF PRESSURE PULSES TO AN INNOVATIVE TURBINE BLADE FILM COOLING SYSTEM

Siegfried Moser, Herbert Jericha, Jakob Woisetschläger, Arno Gehrer, Werner Reinalter  
Institute for Thermal Turbomachinery and Machine Dynamics  
Technical University Graz  
Inffeldgasse 25  
A-8010 Graz / Austria

### ABSTRACT

The evolution of increasing turbine inlet temperature has led to the necessity of full-coverage film cooling for the first turbine vane and blade. This paper deals with the investigation of the aerodynamic behaviour of the transonic wall film on a leading edge with and without leading edge pressure waves. Here these films are used for turbine blade cooling. The pressure waves are produced with a rotating „Pressure Wave Generator“. The numerical simulations have been realised with a commercial CFD-Program. The experimental data were obtained in a linear cascade.

### NOMENCLATURE

#### Symbols

BR	blowing ratio = $(\rho_c v_c)/(\rho_g v_g)$
L	chord length [m]
M	Mach number
m	mass flow [kg/s]
p	pressure [bar]
$\hat{p}$	pressure at shock wave [bar]
T	total temperature [K]
Tu	turbulence level [%]
t	time [sec]
v	velocity [m/s]
x	chordwise co-ordinate [m]
$\rho$	density of main flow [kg/m <sup>3</sup> ]
$\gamma$	shock wave angle [°]
k	ratio of specific heats

#### Indexes

c	coolant flow
g	main flow
w	stagnation condition
p	pulsator flow
s	condition on surface

### INTRODUCTION

One way to improve efficiency in modern gas turbines is to increase the turbine inlet temperature. Additionally modern turbines are designed for increasing mass stream and pressure ratio in the turbine stages leading to transonic conditions in these machines. These conditions lead to pronounced shock systems interfering with the cooling films covering the blade surfaces.

Therefore, an improved cooling system not only has to have high cooling efficiency keeping the increased blade temperature distribution on a uniform level to ensure high reliability and prolong the thermal fatigue life. It also has to have high resistance against high free stream turbulence and shock waves in transonic gas turbines.

The innovative cooling system developed at the Institute for Thermal Turbomachinery and Machine-Dynamics at Technical University Graz promises several new features in meeting the objectives.

Originally this cooling system was intended for industrial steam injected gas turbine cogeneration systems where steam at low temperature and high pressure is available [8], [9], [10], but the application to a gas turbine cycle using air as cooling medium is under discussion.

The characteristic of this cooling method proposed is a cooling film making use of the behaviour of underexpanded jets. An underexpanded jet means a jet from a choked convergent nozzle where the flow subsequently expands supersonically because the external pressure is below the critical value [1], [2], [3]. These jets have a strong tendency to bend towards a convex surface. Previous experimental investigations [4], [5], [6] with this type of cooling film in the leading edge area showed a coolant film coherently covering the surface with a strong adherence to it. Consequently in a next step the influence of strong upstream flow distortions had to be investigated, especially in the leading edge area.

Fig. 1 shows the experimental and calculated results of the attached transonic cooling jet on the leading edge.

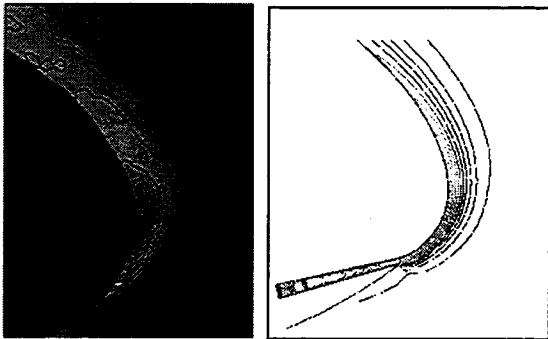


Fig. 1: Density isolines. The digital evaluation of density from holographic interferograms (left [5]) is compared with a numerical calculation using AVL-List FIRE software.

In this work the innovative cooling system was tested for its aerodynamic behaviour on the leading edge in a linear cascade under the influence of pronounced pressure waves to show the resistance to lift off of the cooling jet against high free stream turbulence or shock waves such as vane tail shock in a transonic turbine stage.

**THEORY**

The pressure ratio in shock waves is a function of Mach number and angle, given by velocity and shock wave direction, as given by gas dynamic theory according to [7]:

$$\frac{\hat{p}_w}{p_w} = \frac{\hat{\rho}_w}{\rho_w} = \left[ 1 + \frac{2\kappa}{\kappa+1} (M_n^2 - 1) \right]^{\frac{-1}{\kappa-1}} \left[ 1 - \frac{2}{\kappa+1} \left( 1 - \frac{1}{M_n^2} \right) \right]^{\frac{-\kappa}{\kappa-1}}$$

with  $M_n = M \sin \gamma$

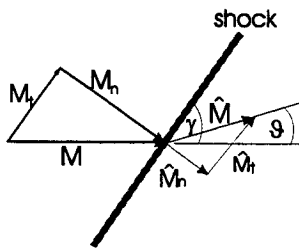


Fig. 2: Oblique shock wave schematic [7]



Fig. 3: Schlieren representation of a trailing edge shock system in the Institute's cascade test rig.

Fig. 3 shows a Schlieren picture of a trailing edge shock system. As an example the determined pressure ratios  $\hat{p}_w/p_w$  for a transonic shock system are given in diagram fig.4. This gives an idea of pressure fluctuations expected in the trailing edge area of the vanes preceding a film cooled turbine blade stage.

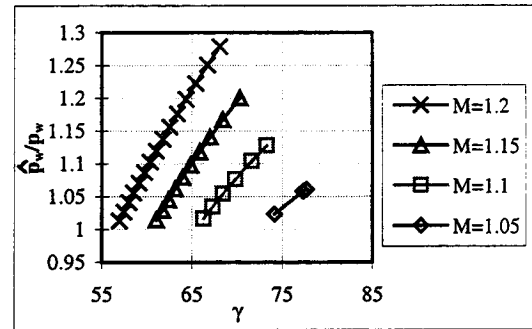


Fig. 4: Pressure ratio between maximum pressure in the shock system over total pressure in the main flow  $\hat{p}_w/p_w$

For experimental cascade testing a device had to be designed for creating such pressure waves with a given pressure ratio  $\hat{p}_w/p_w > 1$  at a certain frequency.

For this purpose a specially designed shock wave generator ("Pulsator", Fig.5) was manufactured of two coaxial cylinders. The internal drum with two slits on opposite sides rotates at 3000 rpm. The external cylinder is stationary and has one slit with a Laval-nozzle.

With this configuration a pulsation frequency of  $100 \text{ s}^{-1}$  can be reached. The pressure waves were produced with high pressure air from the institute compressor facility. The design of the slits was based on isentropic calculations in regard of the necessary air pressure level and mass flow. The final arrangement of the pulsator in the cascade is displayed in Fig. 6.

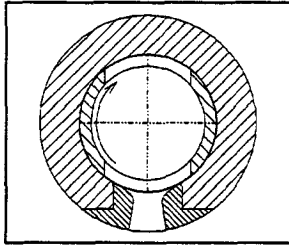


Fig. 5: Schematic drawing of the pressure wave generator

Table 1: Blade and cooling slit geometry [5]

blade chord length	142 mm
blade height	100 mm
pitch/chord ratio	0.694
inlet angle*	55 °
outlet angle*	28 °
slit position (x/L)	0.06
cooling slit length	23.5 mm
slit height	0.2 mm

\*measured from circumferential direction

## MEASUREMENT TECHNIQUES

The total and static pressure of the incoming flow had been measured at several points upstream of the blade cascade at a distance of 150 - 200 mm at various spanwise locations as well as downstream of the blade cascade. While the pressure distribution along the blade surface was measured in groups of ten, the incoming and outgoing flow condition was monitored continuously by a Scanivalve ZOC 14NP/16Px-50 with an electronic multiplex interface and a 486 PC using a National Instruments AT-MIO-16H-9 AD/DA converter board together with Lab View software.

Temperature was measured at several points upstream and downstream by K-type thermoelements together with an amplifier board and was also recorded by the PC based system.

The cooling mass flow was detected using a Fischer & Porter mass flow meter and the corresponding Fischer and Porter software for meter reading correction due to actual pressure and temperature of the CO<sub>2</sub>. The main mass flow was measured using a mass flow nozzle in the main line and with velocity and density measurements upstream of the cascade.

Beside pressure and temperature measurements, flow visualisation was performed by dark field transmission Schlieren technique using a circular Schlieren filter [4]. Due to the circular Schlieren filter density gradients in different directions within the flow field are visualised simultaneously, no direction is missed. As a light source a He-Ne-Laser as well as a white light source (halogen lamp) was used.

For the velocity and turbulence data published in this paper a two channel Laser Doppler Velocimeter (LDV; DANTEC fibre flow, Burst Spectrum Analyser) has been used together with DEHS as seeding material. The mean droplet diameter of this material (produced by PALLAS AGF 5.0 particle generator) was 0.7 µm.

The measurement of pressure waves are executed with two pressure sensors (EPI-411-3.5B +IAM produced by Entran Sensor GmbH) on the leading edge of the cooled blade (Fig. 8).

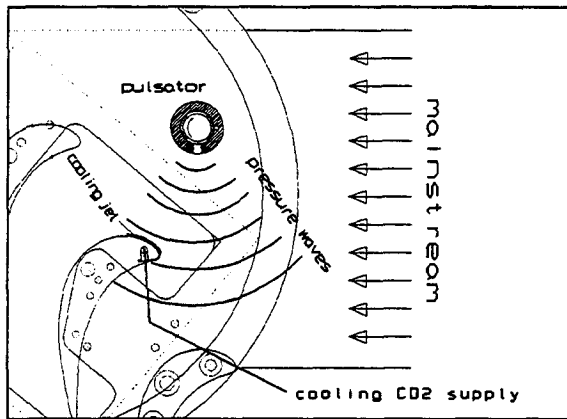


Fig.6: Linear cascade with pulsator

## TEST FACILITY

This experiment was performed in the Institute's cascade test rig being supplied from a continuously running compressor station. From the three compressors available (total engine power 3 MW, volume flow 3000-50.000 m<sup>3</sup>/h) the screw compressor (ATLAS COPCO, 2,6 kg/s maximum mass flow, 3.1 maximum pressure ratio at 400 kW engine power) had been used for the experiments presented here.

A cross section drawing of the investigated blade with cooling slits is given in Fig. 7 and table 1. Cooling slits #2 and #3 are not subject of these investigations. Since it is not possible to run the linear cascade test rig with the same flow temperatures as a real turbine an aerodynamically similar test section was designed using CO<sub>2</sub> as cooling flow medium. A detailed description of the measurement techniques had been given by Woisetschläger et al. [5]

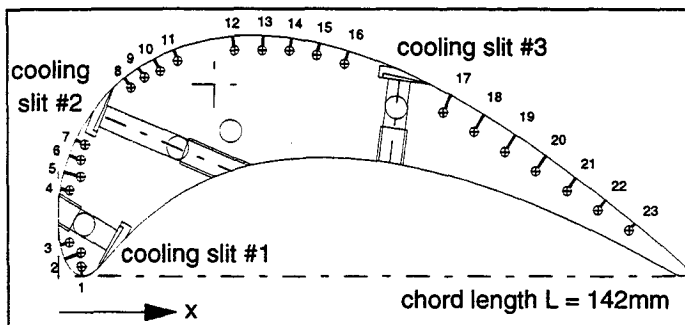


Fig. 7: Geometry of the blade with the position of the cooling slits and pressure taps [5]

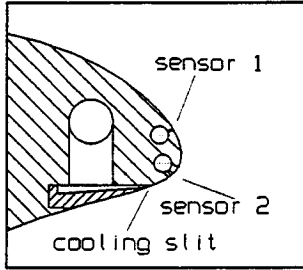


Fig. 8: Pressure sensors placed on leading edge of the cooled blade

### CFD-SIMULATION

With the CFD-software package FIRE (AVL-List Graz) we created a numerical model to simulate the flow field within the test cascade.

**Results with inactive pulsator** At first we simulated the flow field without the pressure wave generator (Fig.9). This results were compared with the flow field including the not working pressure wave generator (Fig.10) to investigate the influence of its geometry on the pressure surface distribution for the blade.

Fig.11 finally displays the Mach number distribution with and without pressure wave generator from the numerical calculations and the experimental data. Fig.11 shows, that the influence of the shock generator geometry to the surface pressure distribution can be neglected.

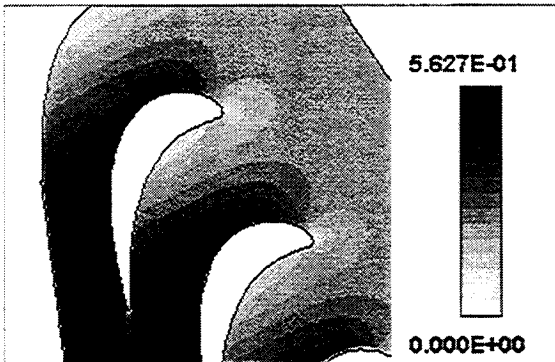


Fig. 9: Calculated test section, no pulsator, mach levels

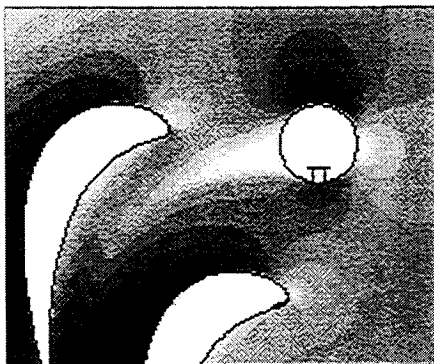


Fig. 10: Calculated test section, with inactive pulsator, mach levels

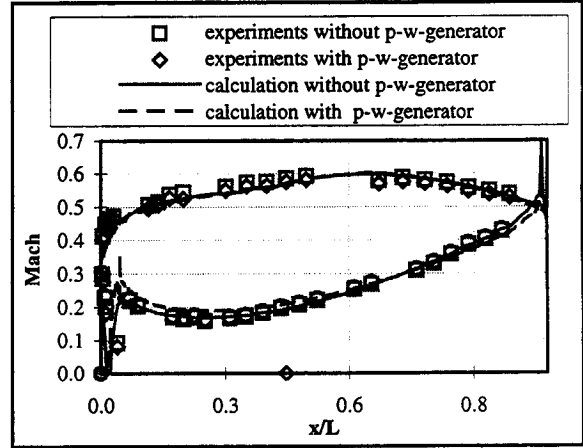


Fig. 11: Mach distribution of blade , calculation, measurements

Table 2, 3 and 4 shows the flow conditions of mainflow and pulsator used for calculation and measurement.

Table 2: Mainflow conditions

MAINFLOW	Inlet	Outlet
total temperature [K]	308	
total pressure [bar]	1.227	
static pressure [bar]		1.01
Tu [%]	3	
Mach number, isen.		0.53
chord Reynolds no.		1.4 E+6
gas		air

Table 3: Cooling jet conditions

COOLANT FLOW	
coolant total temperature [K]	293
coolant total pressure [bar]	2.454
Reynolds number based on throat	9.73E+03
mass rate ( $m_c/m_g$ )	0.002
blowing ratio ( $\rho_c v_c / \rho_g v_g$ )	5.53
injection gas	CO <sub>2</sub>

Table 4: Pulsator inlet conditions

PULSATOR FLOW	
total temperature [K]	293
total pressure [bar]	3.35/3.8
injection gas	air

**Results with active pulsator** Fig. 12 shows the pressure wave transmission as a function of time. The total inlet pressure in the pulsator was fixed with 3.35 bar.

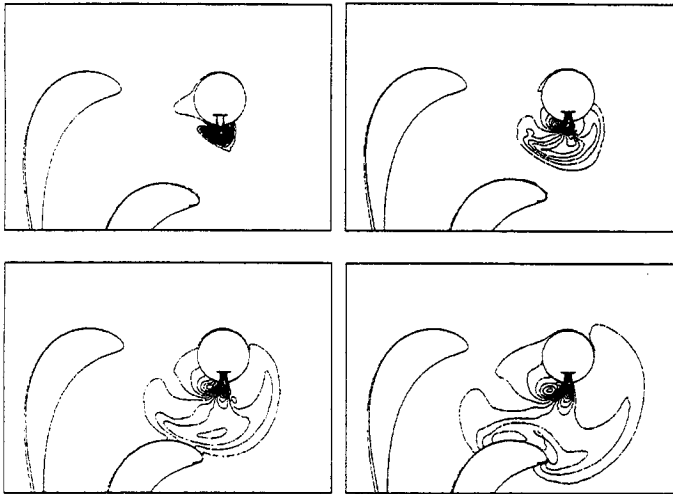


Fig. 12: Pressure wave distribution in test section at four different moments with working pulsator

Fig. 13 shows the pressure distribution at three different instances of time on the surface of the leading edge with working pulsator.

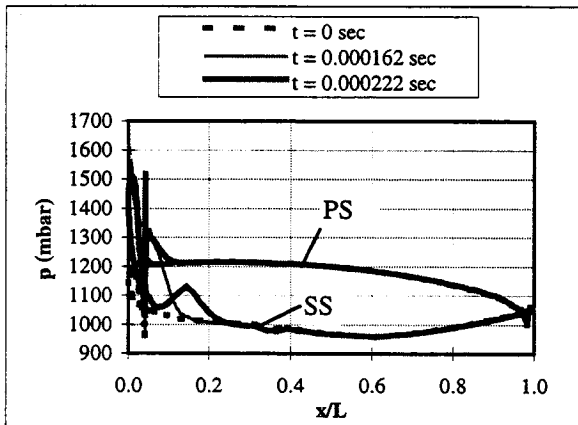


Fig. 13: Pressure distribution on surface of cooled blade ( $p_p=3.35$  bar)

The calculated pressure fluctuation on the leading edge reaches a maximum of 30% of the total pressure in the main flow ( $p_s/p_{gw} \approx 1.3$ ).

## EXPERIMENTAL RESULTS

Fig. 14 presents the time variation of pressure shocks produced by the rotating pressure wave generator at the position of the sensor1 located in the leading edge area (Fig.8). Fig.15 shows the transonic cooling jet visualised using the Schlieren technique and an high speed video camera. The Schlieren pictures clearly show the influence of the periodic pressure changes on the cooling film at the leading edge.

With an pulsator inlet total pressure of 3.35 bar only little influence on the cooling film was recorded. The pressure fluctuation recorded on the surface reached in this case 15 to 25% of the total pressure in the main flow.

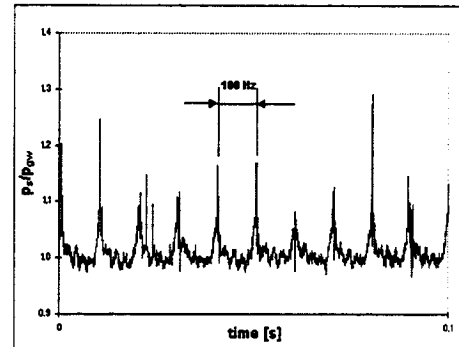


Fig. 14: Time variation of shocks produced by the rotation pressure wave generator at the position of the sensor1 located in the leading edge area ( $p_{cw}/p_g = 2$ ,  $p_{pw} = 3.35$ )

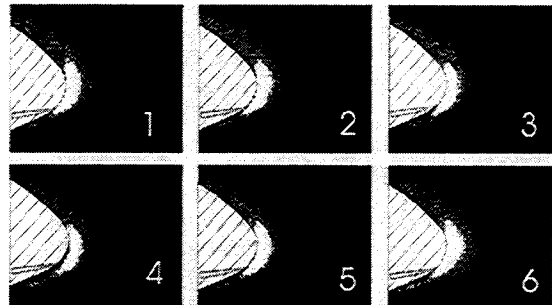


Fig. 15: Schlieren visualisation according to Fig.14 showing only little influence of pressure waves on cooling jet ( $p_{cw}/p_g = 2$ ,  $p_{pw}=3.35$  bar)

In Fig. 16 and 17 the pulsator inlet total pressure was increased to 3.8 bar. Now the pressure ratio between surface static pressure fluctuations and total mainstream pressure exceeded 30%. In this case a temporarily lift-off the cooling jet was observed.

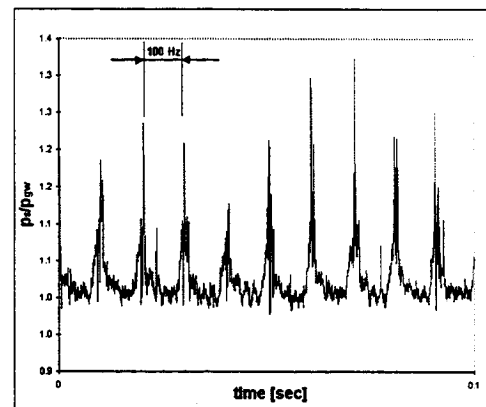


Fig. 16: Time variation of shocks produced by the rotation pressure wave generator at the position of the sensor1 located in the leading edge area ( $p_{cw}/p_g = 2$ ,  $p_{pw} = 3.8$  bar)

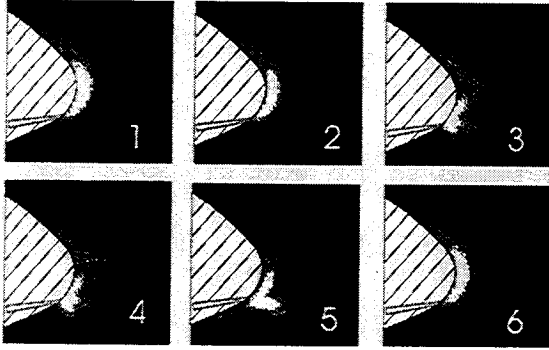


Fig. 17: Schlieren visualisation according to Fig. 16 showing influence of pressure waves on cooling jet showing small temporarily cooling jet „lift offs“ ( $p_{cw}/p_z = 2$ ,  $p_{pw} = 3.8$ )

These results indicate a high resistance of the underexpanded full-coverage cooling jet against pressure waves with pressure ratio  $\hat{p}_w/p_w > 1$ . Thus this innovative cooling system seems to be suitable especially for application in transonic gas turbine stages in which nozzle tail shock waves strike the blade.

## SUMMARY

This investigation together with all previous investigations of the underexpanded cooling film [5] confirms its resistance against high freestream turbulence and shock waves. Ongoing experimental and numerical investigations at Technical University of Graz deal with a film cooling effectiveness study under cascade conditions. First calculations of adiabatic cooling effectiveness are promising and we are going to investigate the innovative cooling system with further experiments.

## ACKNOWLEDGEMENT

The authors gratefully acknowledge the support by the Austrian Science Foundation (FWF) under grant P10698 enabling this research on underexpanded cooling films.

## REFERENCES

- [1] Gilchrist, A. R. and Gregory-Smith, D.G., 1988, „Compressible Coanda Wall Jet: Predictions of Jet Structure and Comparison with Experiment“, International Journal of Heat and Fluid Flow, Vol.9, pp 286-295
- [2] Gregory-Smith D.G. and Gilchrist A.R., 1987, „The Compressible Coanda Wall Jet - an Experimental Study of Jet Structure and Breakaway“, Heat and Fluid Flow, Vol. 8, pp 156-164
- [3] Gregory-Smith D.G. and Hawkins M., 1991, „The Development of an Axisymmetric Curved Turbulent Wall Jet“, International Journal of Heat and Fluid Flow, Vol.12, pp 323-330

- [4] Woisetschläger J., Jericha H., Sanz W., Gollner F., 1995, „Optical Investigation of Transonic Wall-Jet Film Cooling“, ASME COGEN TURBO POWER '95
- [5] Woisetschläger J., Jericha H., Sanz W., Pirker H.P., Seyr A. Ruckebauer T., 1997, „Experimental Investigation of Transonic Wall-Jet Film Cooling in a Linear Cascade“, Turbomachinery-Fluid Dynamics and Thermodynamics, Antwerpen, 1997, pp 447-451
- [6] Gehrler A., Woisetschläger J., Jericha H., 1997, „Blade Film Cooling by Underexpanded Transonic Jet Layers“, International Gas Turbine & Aeroengine Congress & Exhibition, Orlando, 97
- [7] Böls A., Suter P; „Transsonische Turbomaschinen“, 1986, Verlag: G. Braun, Karlsruhe (Wissenschaft und Technik: Taschenbuchausgabe)
- [8] Jericha H., Sanz W., Woisetschläger J., Fesharaki M., 1995, „CO<sub>2</sub>-Retention Capability of CH<sub>4</sub>/O<sub>2</sub>-Fired Graz Cycle“, Proceedings CIMAC 95, paper G07
- [9] Satoh T., Watanabe A., Kajita S., 1991, „Development and Operation of Cheng Cycle Steam Injected Gas Turbine Cogeneration System“, 19<sup>th</sup> CIMAC 1991, paper G22
- [10] Ishizuka T., Suzuki A., 1991, „Steam Injection Aero-derivative Gas Turbine, its Modification Design and Operation Experience“, 19<sup>th</sup> CIMAC 1991, paper G15